Thin Solid Films 545 (2013) 200–204

Contents lists available at ScienceDirect

Thin Solid Films

journal homepage: www.elsevier.com/locate/tsf

Thermoanalytical study of the decomposition of yttrium trifluoroacetate thin films

H. Eloussifi [a,b], J. Farjas [a,*], P. Roura [a], S. Ricart [c], T. Puig [c], X. Obradors [c], M. Dammak [b]

[a] GRMT, GRMT, Department of Physics, University of Girona, Campus Montilivi, E17071 Girona, Catalonia, Spain
[b] Laboratoire de Chimie Inorganique, Faculté des Sciences de Sfax, Université de Sfax, BP 1171, 3000 Sfax, Tunisia
[c] Institut de Ciència de Materials de Barcelona (CSIC), Campus UAB, 08193 Bellaterra, Catalonia, Spain

ARTICLE INFO

Article history:
Received 5 February 2013
Received in revised form 26 July 2013
Accepted 31 July 2013
Available online 7 August 2013

Keywords:
Yttrium trifluoroacetate
Yttria
Thin films
Thermal decomposition
Pyrolysis
Thermal analysis
Thermogravimetry

ABSTRACT

We present the use of the thermal analysis techniques to study yttrium trifluoroacetate thin films decomposition. In situ analysis was done by means of thermogravimetry, differential thermal analysis, and evolved gas analysis. Solid residues at different stages and the final product have been characterized by X-ray diffraction and scanning electron microscopy. The thermal decomposition of yttrium trifluoroacetate thin films results in the formation of yttria and presents the same succession of intermediates than powder's decomposition, however, yttria and all intermediates but YF_3 appear at significantly lower temperatures. We also observe a dependence on the water partial pressure that was not observed in the decomposition of yttrium trifluoroacetate powders. Finally, a dependence on the substrate chemical composition is discerned.

1. Introduction

Among the different routes described for the synthesis of $YBa_2Cu_3O_{7-\delta}$ (YBCO) superconductors, chemical solution deposition (CSD) methods are especially suited for practical purposes since they are flexible, low-cost and scalable [1,2]. In particular, since their early discovery by Gupta et al. [3], yttrium trifluoroacetate ($Y(TFA)_3$), combined with barium and copper TFAs, have been extensively used in the synthesis of high performance YBCO superconducting tapes [4–9]. CSD involves solution preparation, solution deposition and a temperature thermal treatment to remove the organic species and to crystallize the amorphous films.

Thermal analysis (TA) techniques are routinely used to characterize the thermal decomposition of precursors. TA analysis allows us to monitor the evolution of the decomposition under different temperature programs and atmospheres. TA analysis combined with structural characterization provides useful information about the decomposition mechanism as well as its dependence on the treatment conditions [10–15]. Although CSD is used to synthesize thin films, TA studies are customarily carried on powders. The main reason is that the signal in TA measurements is proportional to the sample mass, and thin film masses are at least one order of magnitude smaller than the usual masses of powders. Recent studies have shown that the actual behavior on thin films may significantly differ from that observed on powders [16–19]. The reason is that the transport mechanisms involved on the solid-gas reaction that govern the decomposition process are enhanced on thin films due to the large surface to volume ratio.

The aim of this paper is to analyze the thermal decomposition of yttrium trifluoroacetate ($Y(TFA)_3$) in the form of films, under different conditions of atmosphere, thickness and substrate. Thermogravimetry (TG), differential thermal analysis (DTA), and differential scanning calorimetry (DSC) are used to monitor the decomposition process. The volatiles formed during decomposition are analyzed using evolved gas analysis (EGA) performed with a mass spectrometer. Final and intermediate products are characterized using scanning electron microscopy (SEM) and X-ray diffraction (XRD). We focus our attention on the differences with respect to the behavior reported for powders [20,21]. In particular, we observe that film decomposition starts at a lower temperature than powders. Contrary to powders, the decomposition depends on the water partial pressure and no combustion is observed in films. Finally, decomposition is enhanced for substrates with cation terminations.

2. Experimental details

2.1. Chemicals

Anhydrous $Y(TFA)_3$ with a purity of 99.99% (trace metals basis) was supplied by Aldrich. A solution 0.66 M of $Y(TFA)_3$ in methyl alcohol

* Corresponding author. Tel.: +34972418490; fax.: +34972418098
E-mail addresses: jordi.farjas@udg.cat, jordi.farjas@gmail.com (J. Farjas).

0040-6090/$ – see front matter © 2013 Elsevier B.V. All rights reserved.
http://dx.doi.org/10.1016/j.tsf.2013.07.082

(purity of 99.8%) was obtained at room temperature by manually shaking the mixture for less than 1 min. Films were prepared by manually dropping microdrops (~3 μL) with a micropipette on the surface of a glass disc (12 mm in diameter) or on a square $LaAlO_3$ (LAO) plate (5 × 5 or 10 × 10 mm^2). The solvent was removed by heating the substrate at 70 °C for 15 min in a hot plate under vacuum (pressure around 4.4×10^4 Pa). Nominal film thicknesses were of the order of several hundred nanometers. Nominal thicknesses have been calculated by assuming that the density of pyrolized films is that of bulk yttria (5.01×10^3 kg/m^3), Y_2O_3.

2.2. Characterization techniques

TG and DTA analysis was performed with a Setaram apparatus model, Setsys Evolution 16. To improve the signal–noise ratio, two substrates coated on both sides were analyzed simultaneously. After the experiments, TG and DTA curves were corrected by subtracting a consecutive identical second measurement and by measuring the sample mass at room temperature after the experiment. Gas flow was controlled by mass flow meters. High purity nitrogen, oxygen and synthetic air (impurity level below 5 ppm) at a flow rate around 50 mL/min were used to control the furnace atmosphere. Water-saturated gases were obtained by bubbling the carrier gas in water at standard temperature and pressure (25 °C, 1.013×10^5 Pa). Residual oxygen and water partial pressures on the furnace were below 0.01% and 0.002%, respectively. Oxygen partial pressures were determined using a Roscid Technologies oxygen measuring cell model OxyTrans while water partial pressure was determined by means of an MKS quadrupole mass spectrometer (model Microvision Plus) connected with a steel capillary and a molecular leak to the furnace. EGA analyses were performed by placing the samples inside a quartz tube at a pressure of around 10^{-4} Pa and the volatiles were analyzed using the MKS mass spectrometer. Samples were heated using an external furnace. DSC was performed in a Mettler Toledo DSC model DSC821 with films deposited on a square LAO plate (5 × 5 mm^2) substrate. Thermal analysis experiments were performed at heating rates of 5, 10 and 20 K/min.

XRD experiments were done in a thin film diffractometer PANalytical model X'Pert PRO MRD. The X-ray beam wavelength was 1.5418 Å (Cu-Kα). XRD spectra were analyzed using eva software from SOCABIM and the JCPDS database from the International Centre for Diffraction Data. SEM observations were performed in a Zeiss DSM 960A scanning electron microscope operated at 20 kV. Samples were coated with a thin film of gold to remove electrostatic charges.

3. Results and discussion

Fig. 1 shows the TG curves of $Y(TFA)_3$ thin films in LAO substrates heated at 20 K/min, either in wet or in dry atmospheres, with different oxygen partial pressures, and for similar nominal film thicknesses (around 0.4 μm). In Fig. 1 the measured mass is normalized to the mass after dehydration. As a reference the expected masses of intermediate and final products are plotted as dashed lines. To facilitate the comparison between powders and films, the decomposition of $Y(TFA)_3$ in the form of powders has also been included in Fig. 1.

The overall precursor decomposition can be divided in four stages, labeled as (I) to (IV). The first stage ends at 150 °C and corresponds to the dehydration. Dehydration of anhydrous $Y(TFA)_3$ is related to the water uptake at room temperature of $Y(TFA)_3$ due to its high hygroscopicity [22]. Stages (II) to (IV) involve the formation of intermediates YF_3, $Y_6O_5F_8$, YOF and the final product Y_2O_3. Intermediates and final product have been identified by XRD, Fig. 2. Precisely, after stage II at 450 °C only YF_3 is identified. Above 500 °C, YF_3 decomposes to form $Y_6O_5F_8$ and YOF, at 650 °C no YF_3 is detected, instead $Y_6O_5F_8$ and YOF are identified and at 730 °C traces of $Y_6O_5F_8$, YOF and Y_2O_3 are observed.

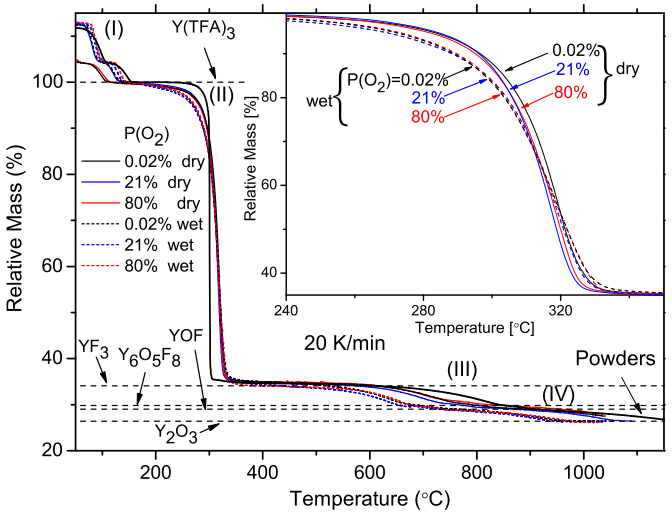

Fig. 1. TG curves for thermal decomposition of $Y(TFA)_3$ films, deposited over LAO substrates. Inset: detail of the precursor film decomposition. *Horizontal dashed lines*: expected masses for the formation of final and intermediate products.

Finally, YOF decomposes to form Y_2O_3, at 950 °C only Y_2O_3 is observed. In Fig. 1 we have plotted (horizontal dashed lines) the expected masses for the formation of YF_3 (34.1%), $Y_6O_5F_8$ (29.8%), YOF (29.0%) and Y_2O_3 (26.4%). From, Fig. 1, one can observe that at the end of each stage, the mass of the solid residues coincides with the expected masses of the intermediates and final products. This sequence of intermediates coincides with those reported in powders [21].

3.1. Decomposition of $Y(TFA)_3$, stage II

Stage II is the main decomposition step; involves the larger mass loss and results in the formation of YF_3. The formation of YF_3 is due to the high electronegativity of fluorine which displaces the oxygen bonded to Y [5]. From the EGA analysis in vacuum, Fig. 3, one can observe that the main volatiles formed during stage (II) coincide with those reported for powders [20,21]; namely CO, CO_2 and $(CF_3CO)_2O$:

$$Y(OOCCF_3)_3 \rightarrow YF_3 + (CF_3CO)_2O + CO + CO_2 \quad (1)$$

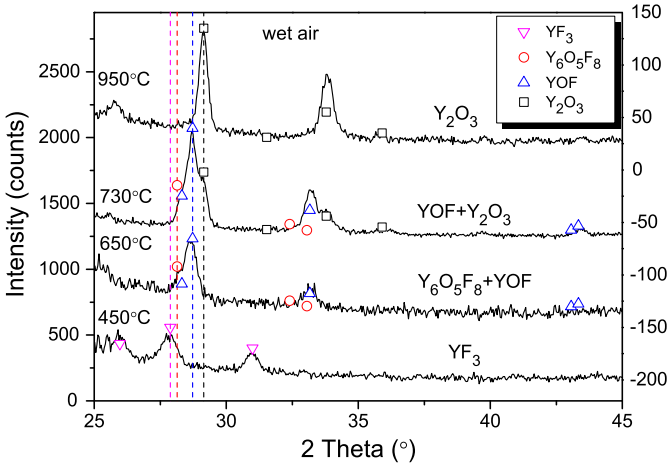

Fig. 2. X-ray curves of the $Y(TFA)_3$ films, deposited over LAO substrates and heated at 20 K/min up to several temperatures.

the presence of $(CF_3CO)_2O$ is identified through the fragments $[CF_3]^+$ and $[CF_3CO]^+$. Moreover, in the absence of water $(CF_3CO)_2O$ decomposes to form CF_3CFO, COF_2 and CO:

$$(CF_3CO)_2O \rightarrow CF_3CFO + COF_2 + CO \quad (2)$$

The latter reaction accounts for the larger amount of CO when compared to CO_2 and the presence of fragments $[CFO]^+$, $[CF]^+$ and $[CF_2O]^+$ in Fig. 3 [21].

Simultaneous TG-DTA, Fig. 4, confirms that the decomposition is an exothermic process. The enthalpy, measured by DSC, is -220 ± 50 J/g and is in agreement with the enthalpy measured in powders in inert atmosphere [21]. Thus from XRD, EGA and DSC we conclude that the decomposition mechanism is the same in powders than in films.

The enthalpy measured in powders was sensitive to the atmosphere; in the presence of oxygen the enthalpy was larger and the DTA peak was not correlated to the mass loss rate signal. This extra contribution in the presence of oxygen is related to the combustion of CO released in reaction (1). This combustion heats the solid sample, but takes place in the gas phase, i.e., it does not affect the mass of the solid residue, thus DTA and TG signals are not correlated [11]. In the case of films, no dependence of the enthalpy on the oxygen partial pressure is observed and the DTA and mass loss rate signals are always correlated, see Fig. 4. This result indicates that there is no effect related to the CO combustion in films. In films, the large surface to volume ration enhances CO removal when compared to the powders, where gas stagnation occurs inside the crucible and in the voids between particles.

The enhanced removal of gaseous reaction products in reactions (1) and (2) is also responsible for the lower temperature onset of the $Y(TFA)_3$ decomposition (in powders gas stagnation may significantly slow down the reaction kinetics [23]). Indeed, in the case of powders, after dehydration, the mass remains constant for a temperature interval of around 150 °C before the decomposition onset (Fig. 1), while in the case of films, the mass continues to decrease after dehydration but at a lower rate, i.e., dehydration and decomposition processes overlap. Despite the fact that films start to decompose at a lower temperature, the second stage of decomposition ($Y(TFA)_3$ decomposition) is completed first in powders than in films (see Fig. 1). The reason is that in powders the low thermal diffusivity of the material and the exothermic nature of the reaction results in a thermal runaway that builds up a fast propagation combustion front. The very abrupt mass loss (Fig. 1) as well as the sharp DTA peak (Fig. 6 in ref. [21]) observed in powders are typical features of the formation of a combustion front. In the case of films, heat removal is clearly enhanced and combustion is prevented. As a result, the mass evolution is smoother, the mass loss rate is lower and decomposition is completed at a higher temperature. Numerical integration of the heat propagation in $Y(TFA)_3$ powders and films confirms, respectively, the presence and absence of a combustion front [17].

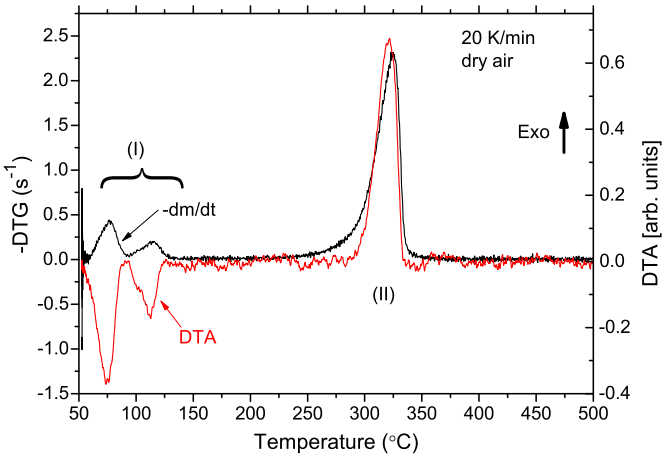

Fig. 4. Simultaneous TG-DTA analysis of thermal decomposition of $Y(TFA)_3$ films, deposited over LAO substrates, in dry synthetic air ($P(O_2) = 21\%$). Heating rate is 20 K/min and the nominal film thickness is 0.39 μm.

Previous results in powders [20,21] indicate that precursor decomposition does not depend on the oxygen and water partial pressures. This result is in agreement with the fact that neither oxygen nor water is involved in reaction (1). From the inset of Fig. 1, one can confirm that $Y(TFA)_3$ decomposition in films does not depend on oxygen partial pressure but does depend on water partial pressure. Actually, from the inset in Fig. 1, one can observe that at the early stages, decomposition is enhanced in the presence of water. This dependence on the water partial pressure was not observed in powders due to their significantly longer diffusion path. To highlight the effect of water diffusion in Fig. 5 we have plotted the evolution of the decomposition of $Y(TFA)_3$ in wet conditions for different film thicknesses; the thicker the film, the higher the decomposition temperature,

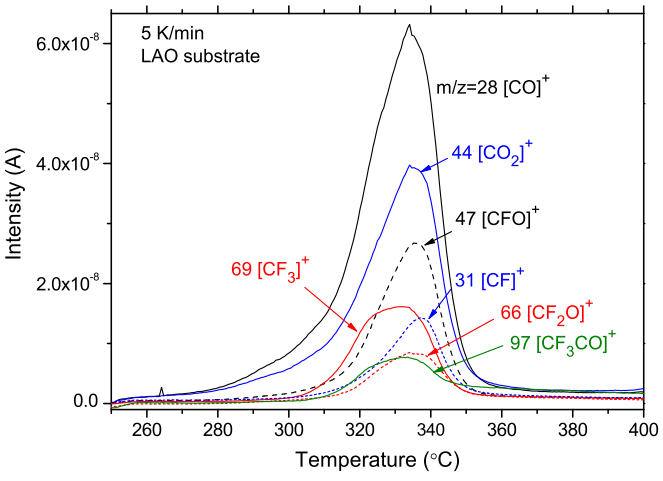

Fig. 3. EGA analysis of thermal decomposition of $Y(TFA)_3$ in vacuum (10^{-4} Pa) for a film deposited on a LAO substrate of nominal thickness 0.95 μm. Heating rate is 5 K/min. Only the more intense ions have been plotted.

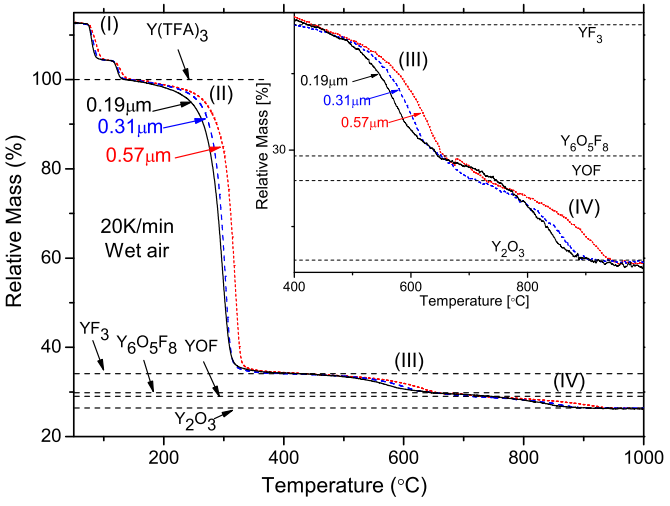

Fig. 5. TG curves for thermal decomposition of $Y(TFA)_3$ of films, deposited over LAO substrates, of different thicknesses heated at 20 K/min in wet synthetic air ($P(O_2) = 21\%$). Inset: detail of last stages of film decomposition.

thus the lower the water contribution. This dependence on the film thickness is not observed in dry atmospheres.

In Fig. 6 we have plotted the evolution of $Y(TFA)_3$ decomposition in films deposited over LAO and glass substrates. From Fig. 6, one can state that decomposition is enhanced in the case glass substrates. To disclose the effect of the chemical properties of the substrate surface, we have analyzed the decomposition of $Y(TFA)_3$ under the same conditions but with two glass substrates submitted to an acid and basic chemical etching respectively, see Fig. 6 (chemical etching: room temperature, 0.1 M NaOH and 0.1 M HCl solutions). When compared to the basic etching, the acid etching clearly shifts the decomposition to lower temperatures. Thus, the cation and H^+ terminations of the bare glass and acid etched glass substrates enhance the decomposition of $Y(TFA)_3$. Consequently, the decomposition enhancement observed in the presence of water is also related to the presence of H^+. Since EGA analysis does not reveal any effect on the gas evolved composition due to water, the presence of water does not modify the decomposition mechanism, reaction (1). Actually, it is very reasonable to assume that the presence of cations weakens the bond between Y^+ and the TFA^- groups, as a result, the decomposition takes place at lower temperature.

The fact that water diminishes the precursor stability together with the slow water diffusion provides an explanation to the fact that no stable anhydrous intermediate is formed during $Y(TFA)_3$ hydrate decomposition [20] and the impossibility to obtain anhydrous $Y(TFA)_3$ by means of a thermal treatment (precursor decomposition starts before the complete removal of water [22]). $Y(TFA)_3$ is very hygroscopic and takes up water very easily when exposed to ambient conditions. Therefore, thermal dehydration is also observed in anhydrous $Y(TFA)_3$, even if they are exposed to ambient conditions for a short time. However, in this case, during the thermal treatment a stable anhydrous intermediate is formed after dehydration [21]. During dehydration, $Y(TFA)_3$ hydrate releases approximately 3.7 water molecules per yttrium atom [20,22], while anhydrous $Y(TFA)_3$ releases 3.0 water molecules per yttrium atom [21]. This extra amount of water present in $Y(TFA)_3$ hydrate is probably responsible for the lower stability of this precursor. Moreover, long time exposure of anhydrous $Y(TFA)_3$ to ambient conditions may result in a significant water uptake that could affect the precursor stability. It is well-known that a large water content in YBCO TFA precursors has a harmful effect on the final properties of the YBCO films [24]. The lower stability of $Y(TFA)_3$ in the presence of water may help to disclose the detrimental effect of the initial water content in the precursor.

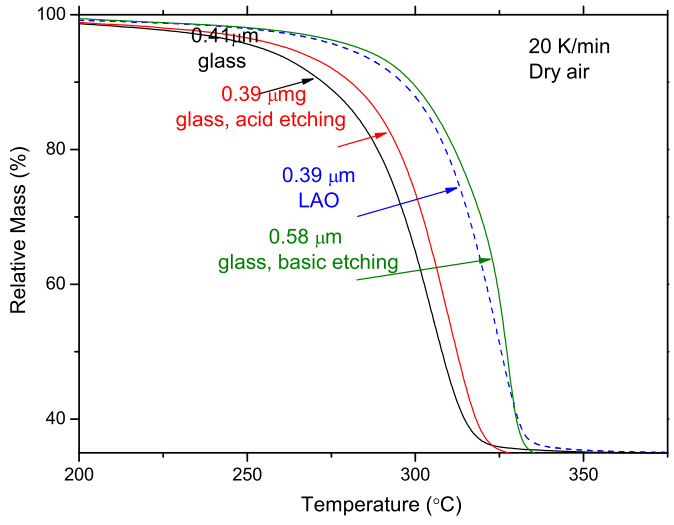

Fig. 6. TG curves for thermal decomposition of $Y(TFA)_3$ of films, deposited over different substrates, heated at 20 K/min in dry synthetic air ($P(O_2) = 21\%$).

3.2. Decomposition of YF_3 and formation of Y_2O_3 stages III and IV

From Figs. 1 and 2 one can observe that YF_3 decomposes to form non-stoichiometric yttrium oxyfluoride $Y_6O_5F_8$, stoichiometric YOF and finally yttria Y_2O_3. Compared to the decomposition of $Y(TFA)_3$, the decomposition rate of YF_3 is much slower, it covers a temperature interval larger than 600 °C. Noteworthy is the fact all intermediates and yttria are formed at significantly lower temperatures in films than in powders (see Fig. 1), e.g., in wet air the transformation of $Y(TFA)_3$ into yttria is completed at 950 °C in films and at 1200 °C in powders. This result indicates that the reaction is probably controlled by diffusion of a volatile reactive or product. From Fig. 1 one can observe that the decomposition is clearly enhanced in the presence of water while no significant dependence on the $P(O_2)$ is observed. Besides, it has been reported that fluoride decomposition is controlled by HF diffusion [5,25,26], therefore we propose the following three step decomposition route:

$$6YF_3 + 5H_2O \rightarrow Y_6O_5F_8 + 10HF \quad (3)$$

$$Y_6O_5F_8 + H_2O \rightarrow 6YOF + 2HF \quad (4)$$

$$2YOF + H_2O \rightarrow Y_2O_3 + 2HF \quad (5)$$

To confirm that reactions (3) to (5) are controlled by diffusion, in the inset of Fig. 5, we have plotted the evolution of YF_3 for three films of different thicknesses. One can verify that for reactions (3) to (5), the thicker the film, the higher the decomposition temperature.

When compared to powders, the temperature decomposition onset in films shifts down about 250 °C. This result indicates that gas transport and renewal are critical parameters in the decomposition of YF_3 and that in the case of solid gas reactions the decomposition temperatures observed in powders strongly differ from the actual decomposition temperature in films. Although YF_3 decomposes at a significantly lower temperature in films, its decomposition is still too high to understand the YBCO formation. It has been proposed [3,7] that after precursor decomposition, a barium yttrium fluoride is formed that will decompose at a much lower temperature allowing the formation of YBCO.

SEM and optical microscopy analyses (not shown) of the films obtained under different atmospheres have revealed that the film thickness is inhomogeneous, in particular the central region is quite flat but thickness at the rim of the film may be as twice as that of the central region. This fact is characteristic of the drop deposition method and it is related to the enhanced solvent evaporation at the rim of the deposited layer: the so-called "coffee ring effect" [27–29]. In addition SEM analysis, Fig. 7, shows that Y_2O_3 films have a similar morphology than powders [21]. It consists in a granular structure of sintered spherical particles. The size of particles is about 150 nm. Film porosity is very high, as a result, the actual thicknesses are about two times the nominal ones. For instance, in Fig. 7.b the calculated nominal thickness is approximately 1 μm while the film thickness is about 2 μm.

4. Conclusions

We have studied the thermal decomposition of yttrium trifluoroacetate films under different atmospheres. Thermal analysis of films reveals the effect of gas transport on the decomposition behavior, a key aspect of the solid–gas reactions involved in precursor decomposition. For instance, when compared to powders, the larger area to volume ratio significantly enhances gas exchange and diffusion. As

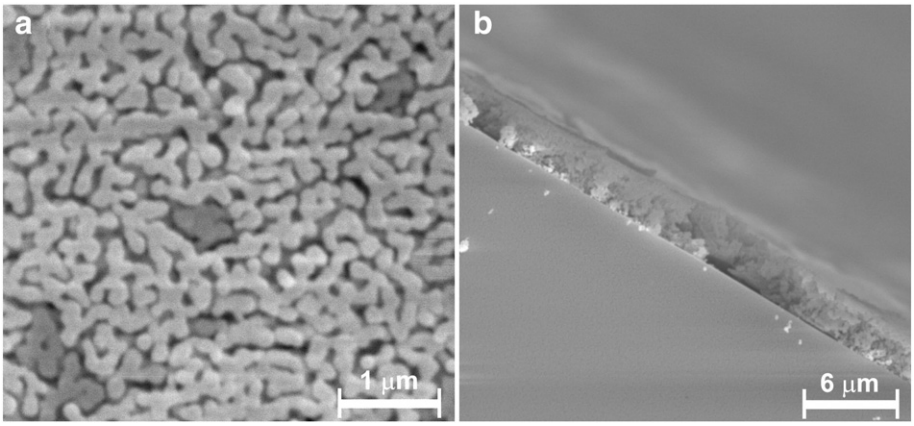

Fig. 7. Scanning electron micrograph obtained when a $Y(TFA)_3$ film deposited over an LAO substrate is heated to 950 °C at a constant rate of 20 K/min in wet air (a) top view (b) cross-sectional view. The nominal film thicknesses is 0.91 μm.

a result, films start to decompose at lower temperatures. In particular, all decomposition steps appear at lower temperatures in films than in powders. This decomposition enhancement results in the formation of yttria in films at 950 °C, i.e., 250° below the yttria formation temperature reported in powders.

The larger area to volume ratio significantly enhances heat transport from the sample to the substrate. Accordingly, during $Y(TFA)_3$ decomposition combustion is prevented. Thus, the decomposition rate of $Y(TFA)_3$ to form YF_3 is much slower in films than in powders.

We have observed that the presence of cations weakens the bond between Y^+ and TFA^- groups. Therefore, films start to decompose at a lower temperature in the presence of water or when they are deposited over substrates with positive ions terminations at their surfaces. In addition, a large initial water content in films or powders reduces the precursor stability.

The decomposition of YF_3 is controlled by HF out-diffusion. Therefore, gas flow, film thickness and water partial pressure are key parameters to control the decomposition kinetics of YF_3.

To sum up, when analyzing solid–gas reactions, the results obtained from powders cannot be extrapolated to films. Besides, thermal analysis on films provides useful information to disclose the reaction mechanisms and to reveal the effect of gas and heat transport on the decomposition behavior.

Acknowledgments

This work was partially funded by the Spanish *Programa Nacional de Materiales* through projects MAT2011-28874-C02-01 and MAT2011-28874-C02-02, by the Consolider program Nanoselect, CSD2007-00041, EU project EUROTAPES NMP3-LA-2012-280432 and by the *Generalitat de Catalunya* contract nos. 2009SGR-185 and 2009SGR-770. H. Eloussifi acknowledges the financial support of the Tunisian Ministry of Higher Education and Scientific Research.

References

[1] R.W. Schwartz, T. Schneller, R. Waser, C. R. Chim. 7 (2004) 433.
[2] V.C. Tung, M.J. Allen, Y. Yang, R.B. Kaner, Nat. Nano 4 (2009) 25.
[3] A. Gupta, R. Jagannathan, E.I. Cooper, E.A. Giess, J.I. Landman, B.W. Hussey, Appl. Phys. Lett. 52 (1988) 2077.
[4] M. Kullberg, M. Lanagan, W. Wu, R. Poeppel, Supercond. Sci. Technol. 4 (1991) 337.
[5] T. Araki, I. Hirabayashi, Supercond. Sci. Technol. 16 (2003) R71.
[6] M.W. Rupich, D.T. Verebelyi, W. Zhang, T. Kodenkandath, X. Li, MRS Bull. 29 (2004) 572.
[7] A. Llordés, K. Zalamova, S. Ricart, A. Palau, A. Pomar, T. Puig, A. Hardy, M.K. Van Bael, X. Obradors, Chem. Mater. 22 (2010) 1686.
[8] M.W. Rupich, X. Li, S. Sathyamurthy, C. Thieme, S. Fleshler, Physica C 471 (2011) 919.
[9] X. Obradors, T. Puig, S. Ricart, M. Coll, J. Gazquez, A. Palau, X. Granados, Supercond. Sci. Technol. 25 (2012) 123001.
[10] M. Mosiadz, K.L. Juda, S.C. Hopkins, J. Soloducho, B.A. Glowacki, Thermochim. Acta 513 (2011) 33.
[11] J. Farjas, J. Camps, P. Roura, S. Ricart, T. Puig, X. Obradors, Thermochim. Acta 521 (2011) 84.
[12] P. Roura, J. Farjas, J. Camps, S. Ricart, J. Arbiol, T. Puig, X. Obradors, J. Nanopart. Res. 13 (2011) 4085.
[13] M. Mosiadz, K.L. Juda, S.C. Hopkins, J. Soloducho, B.A. Glowacki, J. Fluorine Chem. 135 (2012) 59.
[14] J. Farjas, J. Camps, P. Roura, S. Ricart, T. Puig, X. Obradors, Thermochim. Acta 544 (2012) 77.
[15] R. Szczęsny, E. Szłyk, J. Therm. Anal. Calorim. 111 (2013) 1325.
[16] P. Vermeir, I. Cardinael, J. Schaubroeck, K. Verbeken, M. Bäcker, P. Lommens, W. Knaepen, J. D'Haen, K. De Buysser, I. Van Driessche, Inorg. Chem. 49 (2010) 4471.
[17] J. Farjas, D. Sanchez-Rodriguez, H. Eloussifi, R.C. Hidalgo, P. Roura, S. Ricart, T. Puig, X. Obradors, in: M. Jain, X. Obradors, Q. Jia, R.W. Schwartz (Eds.), Solution Synthesis of Inorganic Films and Nanostructured Materials, MRS Symp.Proc., vol. 1449, Cambridge Journals Online, 2012, p. 13.
[18] P. Roura, J. Farjas, S. Ricart, M. Aklalouch, R. Guzman, J. Arbiol, T. Puig, A. Calleja, O. Peña-Rodríguez, M. Garriga, X. Obradors, Thin Solid Films 520 (2012) 1949.
[19] H. Eloussifi, J. Farjas, P. Roura, S. Ricart, T. Puig, X. Obradors, M. Dammak, Thermochim. Acta 556 (2013) 58.
[20] M. Mosiadz, K. Juda, S. Hopkins, J. Soloducho, B. Glowacki, J. Therm. Anal. Calorim. 107 (2012) 681.
[21] H. Eloussifi, J. Farjas, P. Roura, J. Camps, M. Dammak, S. Ricart, T. Puig, X. Obradors, J. Therm. Anal. Calorim. 108 (2012) 589.
[22] S. Mishra, L.G. Hubert-Pfalzgraf, S. Daniele, M. Rolland, E. Jeanneau, B. Jouguet, Inorg. Chem. Commun. 12 (2009) 97.
[23] J. Farjas, A. Pinyol, C. Rath, P. Roura, E. Bertran, Phys. Status Solidi A 203 (2006) 1307.
[24] T. Araki, Bull. Chem. Soc. Jpn. 77 (2004) 1051.
[25] D.E. Wesolowski, M. Yoshizumi, M.J. Cima, IEEE Trans. Appl. Supercond. 17 (2007) 3351.
[26] M. Yoshizumi, I. Seleznev, M.J. Cima, Physica C 403 (2004) 191.
[27] N.D. Denkov, O.D. Velev, P.A. Kralchevsky, I.B. Ivanov, H. Yoshimura, K. Nagayama, Nature 361 (1993) 26.
[28] R.D. Deegan, O. Bakajin, T.F. Dupont, G. Huber, S.R. Nagel, T.A. Witten, Nature 389 (1997) 827.
[29] H. Hu, R.G. Larson, J. Phys. Chem. B 106 (2002) 1334.